Andrew J. Sommese
Department of Mathematics,
University of Notre Dame,
Notre Dame, IN 46556-4618
e-mail: sommese@nd.edu, URL:
http://www.nd.edu/~sommese

Jan Verschelde
Department of Mathematics,
Statistics, and Computer Science,
851 S. Morgan St. (MC 249)
University of Illinois at Chicago,
Chicago, IL 60607-7045
e-mail: jan@math.uic.edu, URL:
http://www.math.uic.edu/~jan

Charles W. Wampler
General Motors R&D Center,
Mail Code 480-106-359, 30500 Mound Road,
Warren, MI 48090-9055
e-mail: charles.w.wampler@gm.com

Advances in Polynomial Continuation for Solving Problems in Kinematics

For many mechanical systems, including nearly all robotic manipulators, the set of possible configurations that the links may assume can be described by a system of polynomial equations. Thus, solving such systems is central to many problems in analyzing the motion of a mechanism or in designing a mechanism to achieve a desired motion. This paper describes techniques, based on polynomial continuation, for numerically solving such systems. Whereas in the past, these techniques were focused on finding isolated roots, we now address the treatment of systems having higher-dimensional solution sets. Special attention is given to cases of exceptional mechanisms, which have a higher degree of freedom of motion than predicted by their mobility. In fact, such mechanisms often have several disjoint assembly modes, and the degree of freedom of motion is not necessarily the same in each mode. Our algorithms identify all such assembly modes, determine their dimension and degree, and give sample points on each. [DOI: 10.1115/1.1649965]

1 Introduction

For many mechanical systems, the set of possible configurations that the links may assume can be described by a system of polynomial equations. In particular, this is true for any mechanism consisting of rigid bodies joined by any of the lower-order pairs, excepting general helical joints. Thus, prismatic, rotary, cylindrical, spherical and planar joints are all allowed. Moreover, many higher-order contact joints are also described by polynomial equations, for example, point-on-plane and line-on-plane contact. We consider both the problem of determining the possible motions of such mechanisms and the problem of finding the parameters of the mechanism such that it meets prescribed precision points. In the latter case, our methods are applicable whenever the governing equations are polynomial in the unknown design parameters.

In the last decade, polynomial continuation developed into a convenient, reliable tool for solving problems in kinematics. It is a numerical process that finds all isolated roots of a polynomial system. (''Isolated'' means there are no other roots in the vicinity, that is, the solution point does not belong to a higher-dimensional solution set, such as a curve or surface.) Starting at the known roots of a suitable start system, the method tracks the solution paths as the start system is continuously transformed into the target system. When the start system and the transformation procedure, called a homotopy, are chosen suitably, the endpoints of these solution paths are guaranteed to include all isolated solutions of the target system. The numerical approach of continuation seems to have been first applied to kinematics in [1,2], as a heuristic, and later by [3] in a modern form with solid mathematical underpinnings. The modern approach, making essential use of complex numbers to avoid singularities or other degeneracies, is presented for engineers and kinematicians in [4,5], where one may find references on the development of the method. (See also [6].) It has proven to be a powerful approach to solving kinematical problems, as exemplified by [7,8,9,10]. The early determinations that the general six-revolute, single-loop spatial mechanism has 16 solutions [3] and the general Stewart-Gough platform has 40 solutions [7] helped guide the subsequent development of algebraic elimination procedures for both problems. When considering a new kinematics problem, Raghavan and Roth [8] recommend to first apply continuation to find the expected number of solutions and use that information to decide if the problem is within range of elimination techniques. Elimination algorithms tend to be faster and to have acceptable accuracy when the number of roots is moderate, but continuation tends to be faster and more accurate when the number of roots is larger. Some publicly available software for polynomial continuation is available [11,12].

It may be that a problem does not have isolated roots, but rather has higher-dimensional solutions. In fact, in general, the solutions of a polynomial system may consist of components of several different dimensions. Simple examples can be constructed as products of polynomials, for example, if $f(x,y)=(x+y-1)(x^2-1)$ and $g(x,y)=(x+y-1)(x-y)$, then the solutions of the system $\{f=0,g=0\}$ consist of the line $x+y-1=0$ and the two points $(x,y)=\pm(1,1)$. It is not necessary that the polynomials be factorizable for these phenomena to arise; in fact, examples of this from kinematics will be presented herein. One, a moveable seven-bar linkage, has both a solution curve and six isolated solutions, and another, a moveable Stewart-Gough platform, has several solution curves. In both cases, the existence of the solution curves depends on the parameters of the linkage having certain special relationships; general linkages of these types have only isolated solutions.

Recently, we developed a method for solving these more general cases by polynomial continuation [13], making essential use of the method described in [14]. Improvements to the technique have been described in [15,16,17]. These are all part of a program of work outlined in [18], which coined the term ''Numerical Algebraic Geometry'' and laid down the basic concepts therein. The algorithm whose use is described in this paper is an extension to [12]; executable code for the experimental algorithms is available at the second author's website and the software is described in more detail in [19].

2 Three Example Problems

In this section, we introduce three example problems: a planar seven-bar structure, a movable Stewart-Gough platform and a problem in spatial body guidance. The solutions to these will be discussed later, after a brief outline of our methods.

2.1 A Seven-Bar Structure. This problem tests a known result from the kinematics of planar linkages. Suppose we are

Contributed by the Mechanisms and Robotics Committee for publication in the JOURNAL OF MECHANICAL DESIGN. Manuscript received July 2002; revised February 2003. Associate Editor: C. Mavroidis.

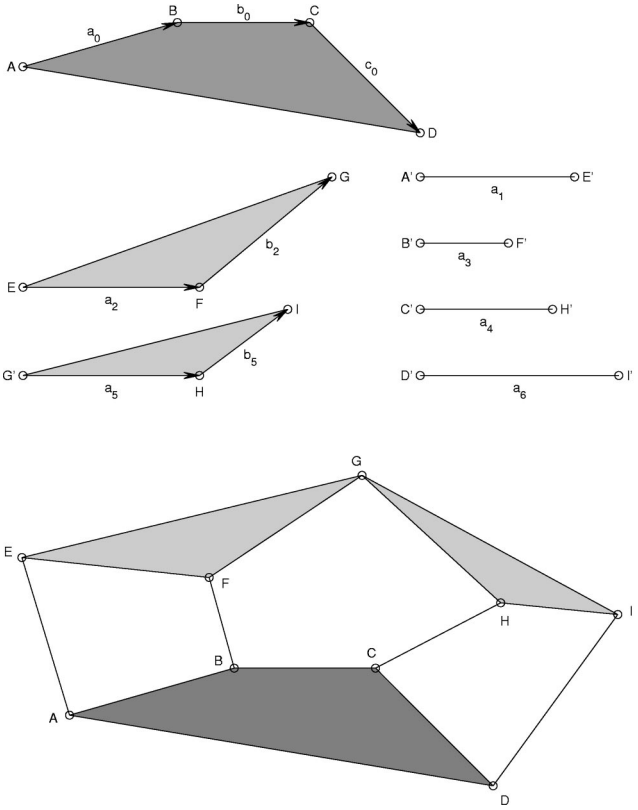

Fig. 1 Top: Find all possible assemblies of these pieces into a 7-bar mechanism. Bottom: One such assembly.

given a collection of seven rigid planar pieces: one quadrilateral, two triangles, and four line segments with vertices labeled as shown at the top of Fig. 1.

We wish to assemble the pieces so as to align A with A', B with B', etc. It is not permitted to flip the pieces over, but they can be translated and rotated in any fashion within the plane. One such assembly is shown at the bottom of Fig. 1. The problem is to find all possible assemblies. It is simplest to hold one of the links, say the quadrilateral, in a fixed location and determine the locations of the remaining links.

Using the formulation in [20] for problems of this type, the problem can be written as a system of polynomial equations:

$$\theta_j \hat{\theta}_j = 1, \quad j = 1, \ldots, 6 \tag{1}$$

$$\begin{aligned} -a_0 + a_1\theta_1 + a_2\theta_2 - a_3\theta_3 &= 0 \\ -b_0 + b_2\theta_2 + a_3\theta_3 - a_4\theta_4 + a_5\theta_5 &= 0 \\ -c_0 + a_4\theta_4 + b_5\theta_5 - a_6\theta_6 &= 0 \end{aligned} \tag{2}$$

$$\begin{aligned} -\overline{a}_0 + \overline{a}_1\hat{\theta}_1 + \overline{a}_2\hat{\theta}_2 - \overline{a}_3\hat{\theta}_3 &= 0 \\ -\overline{b}_0 + \overline{b}_2\hat{\theta}_2 + \overline{a}_3\hat{\theta}_3 - \overline{a}_4\hat{\theta}_4 + \overline{a}_5\hat{\theta}_5 &= 0 \\ -\overline{c}_0 + \overline{a}_4\hat{\theta}_4 + \overline{b}_5\hat{\theta}_5 - \overline{a}_6\hat{\theta}_6 &= 0 \end{aligned} \tag{3}$$

The parameters $a_0, b_0, c_0, a_1, a_2, b_2, a_3, a_4, a_5, b_5, a_6$ are complex numbers that describe the shape of the links. In Eqs. (3), $\overline{a_i}$, $\overline{b_i}$, and $\overline{c_i}$ denote the complex conjugate of a_i, b_i, and c_i. One may notice that the coefficients in Eqs. (3) are the conjugates of those in Eqs. (2). The complex variable $\theta_i = e^{\sqrt{-1}\phi_i}$ represents the rotation of link i through angle ϕ_i. Solutions having $|\theta_i| = 1$ (all

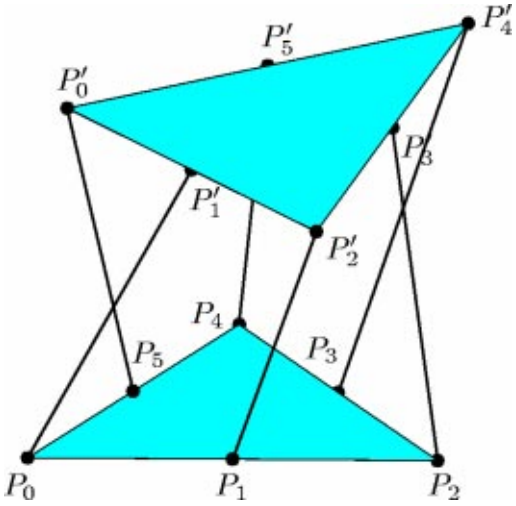

Fig. 2 Griffis-Duffy platform. Both base and endplate are equilateral triangles.

i) mean that the links have real rotation angles, so these correspond to actual solutions of the geometric problem.

For generic parameters, this problem has 18 distinct solutions in complex space, see [21] for a demonstration using a different formulation. For the particular set of pieces shown in Fig. 1, eight of these are "real" solutions having $|\theta_i| = 1$.

For certain special linkages, higher-dimensional solution sets can occur. One such example can be constructed by making the two four-bar linkages ABFEG and CDIHG to be Roberts cognates, ([22], p. 340), so that the solution set must include a four-bar coupler curve, having degree six. Our objective will be to confirm that the known curve is discovered by the algorithm and additionally to see if any other solutions exist.

2.2 Special Stewart-Gough Platforms. A generic Stewart-Gough platform consists of two rigid bodies, called the base and the endplate, joined by six legs. The legs are connected to the base and endplate by spherical joints. As a robot-manipulator, the lengths of the legs are controlled by actuators to move the endplate with six degrees of freedom, but when the leg lengths are held constant, the platform is in most cases a rigid structure. However, for certain arrangements of the joints and certain leg lengths, the structure may lose rigidity and become mobile. For a robot-manipulator, this is generally undesirable and possibly dangerous. On the other hand, the same arrangement might be useful as a mechanism, having one or more degrees of freedom.

When the six ball joints in the base and the six ball joints in the endplate are in general position, a Stewart-Gough platform has forty isolated solutions. This was first established nearly simultaneously by continuation [7], by computer algebra [23,24], and by proof using algebraic geometry [25]. Simpler analytical proofs came later [26,27]. One formulation of the kinematic equations is as follows, where $(\mathbf{e},\mathbf{g}) \in \mathbb{P}^7$ are Study coordinates for rigid body motion [27]. Here, $\mathbb{P}^7$ means seven-dimensional projective space, which means that $(\mathbf{e},\mathbf{g})$ are a set of eight coordinates whose scale does not matter. (Two sets $(\mathbf{e},\mathbf{g})$ that differ only by a nonzero scale factor represent the same rigid-body displacement.) The first four coordinates, $\mathbf{e}$, are a quaternion that represents orientation and the last four coordinates, $\mathbf{g}$, encode position. Considered as four-vectors, $\mathbf{e}$ and $\mathbf{g}$ must be orthogonal to represent a valid rigid-body displacement. This condition is the first equation in the following system, whereas the other six equations express the constraint imposed by the six given leg lengths:

$$\begin{aligned} \mathbf{e}^T\mathbf{g} &= 0 \\ L_0\mathbf{e}^T\mathbf{e} - \mathbf{g}^T\mathbf{g} &= 0 \end{aligned} \tag{4}$$

$$\mathbf{e}^T A_i \mathbf{e} - \mathbf{e}^T B_i \mathbf{g} = 0, \quad i = 1, \ldots, 5$$

Here L_0 is the length of one of the legs, and the 4×4 matrices A_i and B_i depend on the ball joint positions and leg lengths as detailed in [27].

One special kind of Stewart-Gough platform, shown in Fig. 2, is called a Griffis-Duffy platform [28,29]. In this platform, the base and endplate are triangles, with ball joints at each vertex and along each side. The legs connect a side point of one body to a vertex of the other, correspondences proceeding in order around the respective triangles. That is, labelling the joints as $P_0, \ldots, P_5$ clockwise around the base triangle and the corresponding joints of the endplate as $P'_0, \ldots, P'_5$, leg i connects P_i to P'_{i+1}, considering $P'_6 \equiv P'_0$.

We consider two special Griffis-Duffy platforms, first identified in [29]. In the first specialization, the base and endplate triangles are equilateral and the ball joints on the sides are at the midpoints. Figure 2 is of this type. Note that the endplate and base are similar but may have different scales. The second case, a further specialization of the first one, is to make the base and endplates congruent and to make all six leg lengths equal. For convenience, let us call these two special cases the Griffis-Duffy I and Griffis-Duffy II platforms.

Griffis-Duffy I platforms are members of a class of Stewart-Gough platforms that are called *architecturally singular*. For general leg lengths, these platforms have no solutions: they cannot be assembled. However, if one specifies a general position of the endplate with respect to the base and sets the leg lengths to match, then the platform has one-degree-of-freedom of motion. In [29], the motion of Griffis-Duffy I and II platforms are analyzed. We treated both these cases numerically, expecting only to confirm the results in [28]. However, we found instead several surprises that we explain in §4 below.

2.3 A Spatial Body-Guidance Problem. Our final example problem concerns the synthesis of a mechanism to guide a rigid body through six spatial positions. The spatial problem may be regarded as a generalization of the classical planar Burmester problem: given five placements of a moving body in the plane, find the points of the moving body that lie on a common circle fixed in the plane. These points are called ''circle points,'' and the centers of the fixed circles are called ''center points.'' There are in general four centerpoint/circle-point pairs. If we specify only four placements instead of five, we get a center-point curve and a circle-point curve, each of which are cubic [22]. These curves are useful for designing a four-bar linkage to carry the body through the specified locations: a so-called body-guidance design problem.

A related problem, due to Schönflies, considers a body moving in space rather than in the plane, and asks for points of the body that lie on a common fixed sphere for several given placements of the body in space. Seven general positions determine 20 center-point/sphere-point pairs, a result proven by Schönflies in 1886 [22]. Solutions computed by continuation were reported in [5], and a reduction to a degree-20 polynomial in one variable given in [30]. These solutions can be useful for designing a seven-bar spatial mechanism to guide a body through the specified precision points.

We consider a variation of this problem in which only six placements are given. For general positions, these will determine a center-point curve and a corresponding sphere-point curve. Properly speaking, letting $y \in \mathbb{R}^3$ be the center point and $x \in \mathbb{R}^3$ the corresponding sphere point, there is a single center-point/sphere-point curve in (x,y). Projecting this curve onto y only gives the center-point curve in the fixed space, and projecting onto x gives the sphere-point curve in the moving body. It is natural to wonder if the center-point/sphere-point curve is a single irreducible piece and to determine its degree.

For $i = 1, \ldots, 6$, let $p_i \in \mathbb{R}^3$ denote the position of the reference point of the body and let $R_i \in \mathbb{SO}(3) \subset \mathbb{R}^{3\times 3}$ be the rotation matrix for the body's orientation. Equations for the system can be written as, for $i = 1, \ldots, 5$, see [5],

$$y^T(R_i - R_0)x + y^T(p_i - p_0) - (p_i^T R_i - p_0^T R_0)x - (p_i^T p_i - p_0^T p_0)/2 = 0. \tag{5}$$

It may be seen from the bilinear structure of this system that slicing the solution curve by adding a single linear equation in (x,y) will yield at most 20 solutions, while slicing it with a linear equation in just x or y alone will yield at most 10 solutions. These follow from the two-homogeneous Bezout numbers for the system, obtained by finding the coefficient of $\alpha\beta$ in $\Pi_{i=1}^6(\deg_x(f_i)\alpha + \deg_y(f_i)\beta)$, where $\deg_x(f_i)$ is the degree of x in equation f_i, and similarly for $\deg_y(f_i)$. For the slice in (x,y), the coefficient of $\alpha^3\beta^3$ in $(\alpha+\beta)^6$ is 20, and for a slice only in x, the coefficient of $\alpha^3\beta^3$ in $\alpha(\alpha+\beta)^5$ is 10. (See [31] for multi-homogeneous Bezout formulas, and see [22, p.138] for an alternative deduction of these degrees.) These represent limits on the degree and bi-degree of the curve, but do not tell us the exact degrees or whether the curve is irreducible. Our methods will determine these questions.

Table 1 Analogy between solutions of univariate polynomials and system of polynomials

Univariate	System
1 equation in 1 variable	n equations in N variables
Solution points	Solution points, curves, surfaces, etc.
Double roots, triple roots, etc.	Sets with multiplicity
Factorization, $\Pi_i(z-a_i)^{\mu_i}$	Irreducible decomposition
Numerical Representation	
Solution points	Witness sets

3 Outline of the Method

Given a system of m polynomial equations in n variables, $f(x): \mathbb{C}^n \to \mathbb{C}^m$, how can we determine the dimensions of its solution components and how can we represent those solutions numerically? First, we must define what we mean by ''components.'' Notice that, even though in kinematics we are generally interested only in real solutions, at this point we are considering the equations over the complexes. This simplifies the problem considerably; we will investigate the computation of real components in the future.

It is well-known from algebraic geometry, that the solution set can be broken up into *irreducible components*. These are the natural pieces into which one would divide up the set: individual points, curves, surfaces, etc. To be more precise, an irreducible algebraic set is one that cannot be expressed as the union of a finite number of proper algebraic subsets. (An algebraic set is the solution set of some system of polynomial equations.) For example, a line is irreducible: it can be considered the union of an infinite number of points or cut up into a finite number of pieces by inequalities, but neither of these violates its irreducibility. On the other hand, the union of two lines or the union of a line and a point distinct from the line are both reducible. The decomposition of a solution set into its irreducible components is analogous to the factorization of a polynomial in one variable: there are a finite number of solution points, although some may appear with multiplicity. A more complete analogy is given in Table 1.

One should note that irreducible components are determined in complex space. The real part of a complex curve may have several disjoint pieces. A familiar example is that a four-bar coupler curve may have two disjoint circuits, but both are part of the same complex coupler curve; that is, both circuits are given by the same sixth-degree coupler curve equation. The exceptions are when the coupler curve equation factors. For example, the coupler curve of

a parallelogram linkage factors into a circle and a fourth-degree curve, and these two pieces are its irreducible components.

A crucial fact used in our algorithms is that an algebraic set S of dimension k in $\mathbb{C}^n$ meets almost every linear subspace of dimension $n-k$ in a nonzero, finite number of points, where the number of points is equal to the degree d of the set. This is where the use of complex space is very useful, because a real algebraic curve in real 3-space might not intersect a given plane, but when extended to their complex counterparts, the two will meet, albeit possibly at complex-valued points. Let L_{n-k} denote the set of all linear subspaces of dimension $n-k$ in $\mathbb{C}^n$. Then, the members of this set that do not meet S in d isolated points are an algebraic subset of L_{n-k}. On the other hand, almost every line in L_{n-k} completely misses any given algebraic set of dimension less than k. Again, the exceptions form an algebraic subset.

In outline, our algorithm [13] computes the irreducible decomposition, using the facts just stated, as follows. Assuming that the given equations are not all identically zero, we start by looking for components of dimension $n-1$. We do so by intersecting the solution set with a randomly chosen line, L. With probability one, this line meets the components of dimension $n-1$ in a finite number of isolated points, which we compute using continuation. We call these points *witness points*. The line misses all lower-dimensional components entirely. We may now move the line around and follow the solution points to collect samples on the solution set. There are several ways to use these samples to identify which witness points belong to the same irreducible components. One is to fit a polynomial to the sample set and check which other witness points satisfy it [13]. Another alternative is the monodromy algorithm [16], which attempts to connect points by a continuation path. A by-product of either technique is the discovery of the degree of each component, which equals the number of distinct witness points found on the component. The component is described by the collection consisting of the system of equations, the slicing line L, the degree d of the component, the d witness points that are the intersection of L with the component. We call this a witness set for the component. This completes the discovery and decomposition of solution sets of dimension
$n-1$.

We may now proceed to dimension $n-2$, this time cutting with a random plane (a member of L_2). With probability one, this will hit the $(n-2)$-dimensional components in a finite number of isolated points and miss the lower-dimensional components. It does, however, intersect the higher-dimensional components. We use a second continuation to get the isolated points, but we may also get some points on the higher-dimensional components. But this is not a problem, since we can use the information already gleaned in the previous round to detect these and cast them out. We then, as before, collect the witness points into irreducible components to complete the work at dimension $n-2$.

The algorithm moves down the dimensions sequentially, until finally, at dimension zero, we find the isolated solutions to the system.

The final output is a list of all irreducible components found at each dimension. For each of these, we have witness points. The number of witness points is equal to the degree of the irreducible component, and they all lie on a common $(n-k)$-dimensional linear subspace. Starting at a witness point, we can, by continuation, move the linear slice to sample as many points as we like from a component. The combination of the linear slice and the witness points that lie on it form a *witness set* for the component.

In the foregoing description of the method, we have skipped over the issue of sets having multiplicity greater than one. These are higher-dimensional analogues of multiple roots of a polynomial in one variable. The interested reader is referred to [13] for details.

In the next few paragraphs, we give some more details about the efficient computation of witness points and about the monodromy method of finding irreducible components.

3.1 Embedding and Cascade. As described above, witness points are found by slicing the solution set with a sequence of random linear spaces of successively higher dimension. These computations can be done completely independently, but it is much more efficient to combine all the slices into a common formulation, called the *embedding*, and proceed from one slice to the next via a *cascade* of homotopies that respect the embedding. This approach is fully presented in [14]. We give only a brief outline here.

Throughout this description we use a subscripting convention that indicates the size of matrices; for example, $A_{m\times n}$ denotes a $m\times n$ matrix with complex entries. If either m or n is less than 1, $A_{m\times n}$ is empty. Matrix $I_{m\times m}$ is the $m\times m$ identity matrix. A boldface letter with a single subscript denotes a column vector.

Suppose we wish to study a system of m polynomials in n variables, $\mathbf{f}_m(\mathbf{x}_n)$. The number of polynomials and variables are not necessarily equal. Let $k=\min(m,n)$, and introduce k "slack variables," $\mathbf{z}_k$, and k homotopy cascade variables, $\mathbf{t}_k$. We can embed all of the slicing operations for generating witness points at every dimension into a single system of equations of the form

$$\mathcal{E}(\mathbf{x}_n,\mathbf{z}_k,\mathbf{t}_k)=\begin{bmatrix}[I_{k\times k}\ \ A_{k\times(m-k)}]\mathbf{f}_m(\mathbf{x}_n)+B_{k\times k}\mathbf{z}_k\\ C_{(n-k)\times n}\mathbf{x}_n+D_{(n-k)\times 1}\\ \mathbf{z}_k+\mathrm{diag}(\mathbf{t}_k)(E_{k\times n}\mathbf{x}_n+F_{k\times 1})\end{bmatrix}=0, \quad (6)$$

where matrices $A_{k\times(m-k)}$, $B_{k\times k}$, $C_{(n-k)\times n}$, $D_{(n-k)\times 1}$, $E_{k\times n}$ and $F_{k\times 1}$ are random with complex entries, and where $\mathrm{diag}(\mathbf{t}_k)$ is a $k\times k$ diagonal matrix with $\mathbf{t}_k$ on the diagonal. Given $\mathbf{t}_k$, this is a system of $n+k$ equations in the $n+k$ variables $(\mathbf{x}_n,\mathbf{z}_k)$. Ignoring the term $B_{k\times k}\mathbf{z}_k$, the first n equations of the embedding are the original polynomials, either squared up via $A_{k\times(m-k)}$ if $m>n$, or sliced down via $C_{(n-k)\times n}$ and $D_{(n-k)\times 1}$ if $m<n$. For the common case of $m=n$, A, C and D are nonexistent. For $m\neq n$, the validity of replacing $\mathbf{f}_m$ by either the squared up or sliced down versions, as appropriate, is discussed in [14,18].

Recall that the witness points for dimension j are obtained as the simultaneous solution of the polynomials $\mathbf{f}_m$ with j additional random linear equations, the slice. In the case $m<n$, we have $n-m$ slice equations built into the embedding. Let

$$\mathcal{E}_j(\mathbf{x}_n,\mathbf{z}_k)=\mathcal{E}(\mathbf{x}_n,\mathbf{z}_k,[1,\ldots,1,0,\ldots,0]), \quad (6)$$

where the initial $j-(n-k)$ elements of $\mathbf{t}_k$ are nonzero. As can be seen by direct substitution into Eq. (6), any solution of $\mathcal{E}_j$ with $\mathbf{z}_k=0$ is a solution of the original system with j additional linear equations; that is, it is one of the witness points we seek. An algorithm for generating all the witness points at every dimension is to first solve $\mathcal{E}_n(\mathbf{x}_n,\mathbf{z}_k)=0$, which means $\mathbf{t}_k=(1,\ldots,1)$, and then follow solution paths in a cascade of k homotopies, each taking one more entry in $\mathbf{t}_k$ from one to zero. At each stage of the cascade, the witness points are those with $\mathbf{z}_k=0$ and the rest are start points for the solution paths for the next stage. This embedding of one slice within another saves considerable computation compared to naively computing each slice independently.

3.2 Monodromy With Linear Traces. With witness points in hand, the next step is to group them into the irreducible components. Irreducible components are the pieces of the solution set that remain connected even after singularities have been removed. The essential fact is that if two irreducible components X and Y of dimension i meet at all, their intersection is of lower dimension: $\dim(X\cap Y)<i$. Suppose we have witness points for X and Y on a common linear slice L of dimension $n-i$, but we don't know which witness point is on which component. We can track the witness points in a continuation as we move L in a general manner. A general motion of L has a zero probability of touching $X\cap Y$, because its dimensionality is too low. So the paths of the witness points for X and those for Y have a zero probability of crossing. The *monodromy* method [16] simply moves the slice L

Table 2 Execution summary for 7-bar mechanism (see text for explanation)

	Witness Generate					Witness Classify		
dim	x	ns	$\hat{W}$	∞	cpu	1	0	cpu
1	48	42	6	0	8.7s	6	0	42.2s
0	42	—	6	36	3.7s	0	6	0.3s
tot	90	42	12	36	12.4s	6	6	42.5s

around randomly generated loops and checks upon return to the initial position whether any of the solution paths ends on a different witness point than it started. If so, we know that the two witness points are on the same irreducible component. After tracking enough monodromy loops, one may hope to discover all possible connections and thereby know how the witness points group into components.

The shortcoming of a naive implementation of monodromy is that one never knows when to terminate. The connections between witness points occur on loops that encircle branch points where two or more witness points coincide or meet the same singularity. Since we do not know at the outset how many irreducible components there are, we do not know from monodromy alone when all connections have been found.

An answer to this problem is to use linear traces [17]. Given a subset of witness points on a component, the trace test tells if the subset is complete. One version of the test is as follows: if we move the slice parallel to itself by varying the constant of one equation of the slice (i.e., an element of $F_{k\times 1}$), the centroid of the complete witness point set for a component must move on a line. Moreover, since the orientation of the slices is general, linearity of the trace implies that the witness set is complete. Thus, by checking the trace after every new monodromy connection is found, we can determine which subgroupings of the witness points form complete irreducible components and only track the incomplete sets in the succeeding monodromy loops. When all the subgroups pass the trace test, the irreducible decomposition is complete. Alternatively, one can check traces on subsets of the witness points to find the irreducible decomposition without monodromy. When the number of witness points is large, this is an intractable combinatoric problem, but after some initial groupings are found by monodromy, the combinatoric approach can be used to finish the task. For a small number of groupings, the combinatoric approach is preferable, since the cost of computing monodromy loops is large compared to the cost of a trace test. The question of deciding when to switch from monodromy to combinatorics is still open for study.

4 Solutions of the Examples

We now return to the sample problems described in §2 and discuss the results found by our algorithms. The timings reported in this paper are obtained from runs on an 800Mhz Pentium III Linux machine.

4.1 A Mobile Seven-Bar Linkage. As described above, we may construct a mobile seven-bar linkage using Roberts cognates. A particular example is as follows. First, choose

$$b_0=0,\quad b_2=-0.11+0.49i,\quad a_2=0.46,\quad a_5=0.41,$$
$$c_0=1.2,\quad \alpha=0.6+0.8i,\quad \beta=e^{1.8i}. \tag{7}$$

Then, derive the remaining parameters as

$$a_3=a_5,\quad \gamma=b_2/a_2,\quad b_5=a_5\gamma,\quad a_0=c_0/\gamma,\quad a_4=|b_2|,$$
$$a_1=|a_0+a_3\alpha-a_4\beta/\gamma|,\quad a_6=|a_4\beta-b_5\alpha-c_0|. \tag{8}$$

The computations for this example begin with a test for a solution curve. To obtain witness points on any motion curves that might exist, we intersect the solution set with a random hyperplane. This means we add a random linear equation to the system and use the homotopy in [14] to find all solution points. The extra equation is incorporated using a slack variable. As indicated in the first line of Table 2, this homotopy requires tracking 48 solution paths (column with header $\boldsymbol{x}$). After 8.7s, we find six witness points and 42 ''non-solutions,'' (column ''ns'' in Table 2). Non-solutions are distinguished from witness points by having a non-zero slack variable. The six witness points represent the sixth-degree coupler motion, which traces the path shown in Fig. 3(*a*). The coefficients of the coupler motion equation are found by sam-

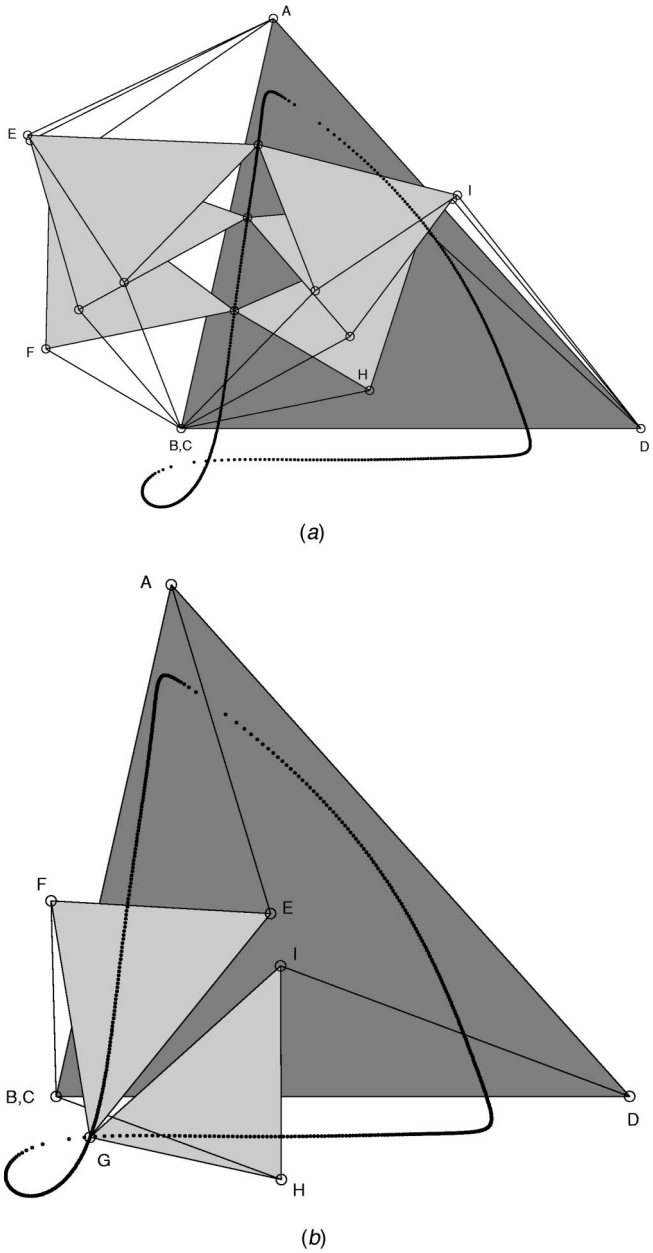

Fig. 3 Assemblies of a seven-bar linkage: (*a*) a solution curve of degree six and (*b*) one of six isolated solutions.

pling and fitting, confirming in the process that no equation of lower than degree six fits the data. In this way, the algorithm confirms that the coupler motion is one irreducible component of degree six. Note that by "coupler motion" we mean the curve $n(\theta_i, \hat{\theta}_i)$, $i=1,\ldots,6$, satisfying Eqs. (1,2,3), which must be distinguished from the "coupler curve," meaning the path traced at by the coupler point.

In the second stage of the algorithm, summarized in line two of Table 2, the 42 non-solutions from the first stage are used as start points for a homotopy that will lead to the isolated roots. After 3.7s, we find that there are six potential witness points (column "$\hat{W}$"), with the other 36 solutions diverging to roots at infinity (column "∞"). Using the coupler motion equation from the first stage, we confirm that none of the six finite points is on the coupler motion, hence they are all true witness points. Each of these is a rigid assembly of the links, one of which is shown in Fig. 3(*b*).

The greatest cost in execution time on this problem was the 42s used to construct an interpolating polynomial for the coupler motion. To only confirm that the six witness points are on one irreducible component, double precision floating-point arithmetic is sufficient. However, to test the solutions at the next stage by the method of [13], we need an accurate interpolating polynomial. For this purpose, we used multi-precision arithmetic routines to compute sample points to 40 decimal places, which is computationally expensive. A more efficient approach [16] is used on the next example problem, but we report here the earlier approach.

The isolated solutions have a simple physical interpretation. Regard the linkage as two four-bars, *ABFEG* and *CDIHG*, joined at a common coupler point *G*. If we disconnect these linkages at the coupler point, both sweep out the same coupler curve. The isolated solutions come where the coupler curve self-intersects, that is, at its double points. Observe that in Fig. 3(*b*), four-bar *ABFEG* is positioned to move horizontally along the coupler curve whereas four-bar *CDIHG* is ready to move along the near vertical portion of the curve. Since these motions are incompatible, the assembled structure is immobile in this configuration. We may reverse the roles to get a second isolated solution at this same double point of the coupler curve. A general four-bar coupler curve has three double points, and since this class of moveable seven-bar structures will have two isolated solutions associated to each double point, there will be in general six isolated solutions. In the example worked here, only one double point is real, hence two of the six isolated solutions are real.

4.2 Griffis-Duffy Platforms. We begin the analysis of the Griffis-Duffy platforms by searching for solution curves. Starting with 128 paths (the total degree of Eqs. (4), the intersection of the curves with a random plane gives forty witness points. Computation of the witness points takes about one minute.

In this example, it is highly desirable to avoid the interpolation step that was so expensive in the seven-bar example. This is because the number of monomials to compute grows exponentially as the dimension and the degree increase. Also, high degree polynomials are numerically difficult, so expensive multi-precision arithmetic is needed. Instead of interpolation, we can apply the monodromy algorithm of [16] to detect irreducible components, using linear traces to validate the groupings [17].

4.3 Griffis-Duffy I. In this case, the monodromy algorithm of [16] predicts that the 40 witness points break into 12 lines and an irreducible curve of degree 28. Monodromy predicts this in 33.4s and linear traces validate the groupings in 4.8s. (For comparison, we also ran the interpolation algorithm and found that it requires 1h 19m to compute an interpolant of degree 28.) The twelve lines all satisfy the equation $\mathbf{e}^T\mathbf{e}=0$, which means that they do not give physically meaningful configurations. This is because **e** is a quaternion representing the rotation of the endplate, and a solution (**e,g**) is meaningful only if it can be rescaled to $\mathbf{e}^T\mathbf{e}=1$. Therefore, we find that the Griffis-Duffy I platform has a single irreducible motion curve of degree 28.

On the face of it, this result seems to be at odds with the result of Husty and Karger [29], who give a degree 20 polynomial that vanishes on the motion curve. However, on closer inspection, there is no contradiction: Husty and Karger first eliminate the positional variables **g** and work only with **e**. We find that the degree 28 curve in the full coordinates (**e,g**) drops to only degree 20 when projected onto the rotational component **e**.

4.4 Griffis-Duffy II. This special case of the Griffis-Duffy I platform also has 12 lines corresponding to degenerate assemblies, but now the curve of degree 28 breaks up into lower-degree irreducible components. It takes 27.6s for the monodromy algorithm of [16] to group the 28 witness points into five sets: four of the five have cardinality six, and one set has four points. Validation of these groups by linear traces takes an additional 4.3s. (Again, purely for purposes of comparison, we also compute interpolating polynomials. This time it is much cheaper, only 2m 34s, because the degree of the components is much lower.)

In this case, the comparison of our results with those in [29] are more striking: we find five components of degree {6,6,6,6,4} whereas Husty and Karger report four components of degree {6,4,4,4}. Two of the differences are resolved similarly as in the Griffis-Duffy I case. That is, we find that two of the quartics reported in [29] are indeed fourth-degree in **e**, but they are degree six in (**e,g**). However, Husty and Karger, working with symbolic computation guided by hand, did not report one of the sextic components. This shows the value of a general algorithm and demonstrates the effectiveness of our numerical approach.

4.5 Center-Point / Sphere-Point Curves. Briefly stated, slicing with a random hyperplane, our approach finds 20 witness points on the center-point/sphere-point curve, which agrees with the degree calculated via the two-homogeneous Bezout number. Using the monodromy algorithm, we find that all 20 solutions connect, so we may conclude that the center-point/sphere-point curve is an irreducible curve of degree 20. Slicing with a hyperplane involving only x gives ten witness points, thus showing that the sphere-point curve is degree 10, and similarly, slicing with a linear equation in only y, we find that the center-point curve is also degree 10. These results confirm that the upper bounds on these degrees predicted from the bi-linearity of Eqs. (5) are exact. One should always keep in mind that calculations of total degree, multihomogeneous degree, and the like, are merely upper bounds on the actual degree of the variety. Our method provides a convenient way to determine the actual degree.

This example illustrates a phenomenon that occurs frequently in kinematics: a projection of an algebraic variety onto a subset of the variables can have a lower degree than the variety itself. We do not need to eliminate variables to answer questions about the projection; we work numerically with all the variables, taking special slices to find the properties of the projection.

5 Conclusions

From the experience of the last decade, polynomial continuation has been known to be a reliable and convenient way to find solutions to problems in kinematics. However, until recently, these methods were limited to finding isolated roots, which limited the kinds of problems that could be addressed. Of particular difficulty are overconstrained mechanisms, which have more degrees of freedom of movement than expected from the usual mobility calculation. These may have a mixture of isolated solutions (rigid assemblies) and motion curves of various dimensions. Also, it can happen that the motion at one dimension is composed of more than one irreducible piece.

We have developed software, well documented in the applied math literature, for solving these more difficult problems. This paper reports on the application of the new methods to several

problems in kinematics: an overconstrained planar mechanism, Griffis-Duffy examples of movable Stewart-Gough platform structures, and center-point/sphere-point curves for six spatial positions. In each case, our numerical methods give a complete irreducible decomposition of the solution set. For the planar seven-bar, the results are consistent with known theory: two Roberts cognate four-bars share a degree-six coupler curve and the three double points of the coupler curve each give two rigid assemblies of the seven-bar. Calculations for the center-point/sphere-point curve also agree with prior theory. However, for the Griffis-Duffy platforms, we get a bit of a surprise: we find some differences from the results published by Husty and Karger. Of these, differences in the degrees of components were not true contradictions, but are due to the use by Husty and Karger of a projection onto rotational coordinates whereas we work the problem in both position and rotation coordinates. However, for the Griffis-Duffy II platform, our algorithm finds a sixth-degree component that they did not report. This shows the usefulness of the numerical approach to find new results or check results found by other means.

Acknowledgments

We gratefully acknowledge the support of this work by Volkswagen-Stiftung (RiP-program at Oberwolfach). The first author thanks the Duncan Chair of the University of Notre Dame and National Science Foundation. This material is based upon work supported by the National Science Foundation under Grant No. 0105653. The second author thanks the Department of Mathematics of the University of Illinois at Chicago and National Science Foundation. This material is based upon work supported by the National Science Foundation under Grant No. 0105739 and Grant No. 0134611. The third author thanks the General Motors Research and Development Center for its support.

References

[1] Roth, B., and Freudenstein, F., 1963, ''Synthesis of Path-generating Mechanisms by Numerical Methods,'' ASME J. Eng. Ind., **85B-3**, pp. 298–306.
[2] Roth, B., and Freudenstein, F., 1963, ''Numerical Solution of Systems of Nonlinear Equations,'' J. Assoc. Comput. Mach., **10**, pp. 550–556.
[3] Tsai, L.-W., and Morgan, A. P., 1985, ''Solving the Kinematics of the Most General Six- and Five-Degree-of-Freedom Manipulators by Continuation Methods,'' ASME J. Mech. Des., **107**, pp. 189–200.
[4] Morgan, A. P., 1987, *Solving Polynomial Systems Using Continuation for Scientific and Engineering Problems*, Prentice-Hall, Englewood Cliffs, NJ.
[5] Wampler, C. W., Morgan, A. P., and Sommese, A. J., 1990, ''Numerical Continuation Methods for Solving Polynomial Systems Arising in Kinematics,'' ASME J. Mech. Des., **112**, pp. 59–68.
[6] Li, T. Y., 1997, ''Numerical Solution of Multivariate Polynomial Systems by Homotopy Continuation Methods,'' Acta Numerica, **6**, pp. 399–436.
[7] Raghavan, M., 1993, ''The Stewart Platform of General Geometry has 40 Configurations,'' ASME J. Mech. Des., **115**, pp. 277–282, June.
[8] Raghavan, M., and Roth, B., 1995, ''Solving Polynomial Systems for the Kinematic Analysis and Synthesis of Mechanisms and Robot Manipulators,'' ASME J. Mech. Des., **117**(B), pp. 71–79.
[9] Waldron, K. J., and Sreenivasen, S. V., 1996, ''A Study of the Solvability of the Position Problem for Multi-Circuit Mechanisms by Way of Example of the Double Butterfly Linkage,'' ASME J. Mech. Des., **118**(3), pp. 390–395.
[10] Wampler, C. W., Morgan, A. P., and Sommese, A. J., 1992, ''Complete Solution of the Nine-point Path Synthesis Problem for Four-bar Linkages,'' ASME J. Mech. Des., **114**, pp. 153–159.
[11] Morgan, A. P., Sommese, A. J., and Watson, L. T., 1989, ''Finding All Isolated Solutions to Polynomial Systems Using HOMPACK,'' ACM Trans. Math. Softw., **15**, pp. 93–122.
[12] Verschelde, J., 1999, ''Algorithm 795: PHCpack: A General-purpose Solver for Polynomial Systems by Homotopy Continuation,'' ACM Trans. Math. Softw., **25**(2), pp. 251–276. Software available at http://www.math.uic.edu/~jan.
[13] Sommese, A. J., Verschelde, J., and Wampler, C. W., 2001, ''Numerical Decomposition of the Solution Sets of Polynomial Systems into Irreducible Components,'' SIAM (Soc. Ind. Appl. Math.) J. Numer. Anal., **38**(6), pp. 2022–2046.
[14] Sommese, A. J., and Verschelde, J., 2000, ''Numerical Homotopies to Compute Generic Points on Positive Dimensional Algebraic Sets,'' Journal of Complexity, **16**(3), pp. 572–602.
[15] Sommese, A. J., Verschelde, J., and Wampler, C. W., 2001, ''Numerical Irreducible Decomposition Using Projections from Points on the Components,'' in E. L. Green, S. Hosten, R. C. Laubenbacher, and V. Powers, ed., *Symbolic Computation: Solving Equations in Algebra, Geometry, and Engineering*, vol. 286 of *Contemporary Mathematics*, pp. 37–51. Amer. Math. Soc.
[16] Sommese, A. J., Verschelde, J., and Wampler, C. W., 2001, ''Using Monodromy to Decompose Solution Sets of Polynomial Systems into Irreducible Components,'' C. Ciliberto, F. Hirzebruch, R. Miranda, and M. Teicher, eds, *Application of Algebraic Geometry to Coding Theory, Physics and Computation*, pp. 297–315. Kluwer Academic Publishers.
[17] Sommese, A. J., Verschelde, J., and Wampler, C. W., 2002, ''Symmetric Functions Applied to Decomposing Solution Sets of Polynomial Systems,'' SIAM (Soc. Ind. Appl. Math.) J. Numer. Anal., **40**(6), pp. 2026–2046.
[18] Sommese, A. J., and Wampler, C. W., 1996, ''Numerical Algebraic Geometry,'' J. Renegar, M. Shub, and S. Smale, eds, *The Mathematics of Numerical Analysis*, Vol. 32 of *Lectures in Applied Mathematics*, pp. 749–763. Amer. Math. Soc.
[19] Sommese, A. J., Verschelde, J., and Wampler, C. W., 2003, ''Numerical Irreducible Decomposition Using PHCpack,'' M. Joswig, and N. Takayama, eds, *Algebra, Geometry and Software Systems*, pp. 109–130, Springer-Verlag.
[20] Wampler, C. W., 1999, ''Solving the Kinematics of Planar Mechanisms,'' ASME J. Mech. Des., **121**, pp. 387–391.
[21] Innocenti, C., 1995, ''Polynomial Solution to the Position Analysis of the 7-link Assur Kinematic Chain with One Quaternary Link,'' Mech. Mach. Theory, **30**(8), pp. 1295–1303.
[22] Bottema, O., and Roth, B., 1979, *Theoretical Kinematics*, North-Holland, Amsterdam.
[23] Lazard, D., 1992, ''Stewart Platform and Gröbner Basis,'' *Proc. ARK*, pp. 136–142, Ferrare, September.
[24] Mourrain, B., 1993, ''The 40 Generic Positions of a Parallel Robot,'' *Proc. ISSAC'93*, pp. 173–182, Kiev (Ukraine), July, ACM press.
[25] Ronga, F., and Vust, T., 1992 ''Stewart Platforms without Computer?'' Proc. Conf. Real Analytic and Algebraic Geometry, Trento, pp. 197–212.
[26] Husty, M. L., 1996, ''An Algorithm for Solving the Direct Kinematics of General Stewart-Gough Platforms,'' Mech. Mach. Theory, **31**(4), pp. 365–380.
[27] Wampler, C. W., 1996, ''Forward Displacement Analysis of General Six-in-Parallel SPS (Stewart) Platform Manipulators Using Soma Coordinates,'' Mech. Mach. Theory, **31**(3), pp. 331–337.
[28] Griffis, M., and Duffy, J., 1993, ''Method and Apparatus for Controlling Geometrically Simple Parallel Mechanisms with Distictive Connections,'' US Patent 5,179,525.
[29] Husty, M. L., and Karger, A., 2000, ''Self-motions of Griffis-Duffy Type Parallel Manipulators,'' *Proc. IEEE Int. Conf. Robotics and Automation*, San Francisco, CA, April.
[30] Innocenti, C., 1995, ''Polynomial Solution of the Spatial Burmester Problem,'' ASME J. Mech. Des., **117**(1), pp. 64–68, March.
[31] Morgan, A. P., and Sommese, A. J., 1987, ''A Homotopy for Solving General Polynomial Systems that Respects m-homogeneous Structures,'' Appl. Math. Comput., **24**, pp. 101–113.